Electronic Supplementary Information

A Stable Ultra-Microporous Hafnium-Based Metal-Organic Framework with High Performance for CO₂ Adsorption and Separation

Yali Ma, Haitang Wang, Hailong Wang, Jiani Wang, Shuaiyu Jiang, Qiang Zheng, Songyan Jia, Xue Li, Tianyi Ma**

Prof. Y. Ma, Dr. H. Wang，Dr. H. Wang, Dr. J. Wang, Prof. Y. Q, Zheng, Prof. Y. Jia Prof. X. Li
College of Chemical Engineering, Shenyang University of Chemical Technology, Shenyang 110142, P. R. China

Prof. T. Ma, Y Jiang
School of Science, RMIT University, Melbourne, VIC 3000, Australia
E-mail: tianyi.ma@rmit.edu.au

S1 Experimental Section

Materials and method

All chemicals were purchased from commercial sources and used without any further purification. Zirconium chloride ($ZrCl_4$, 98 %, Aladdin), N, N-dimethylformamide (DMF, AR, Sinopharm Chemical Reagent Co. Ltd.), Acetic acid (CH_3COOH, AR, Fuyu Reagent), acetonitrile (AR, Fuyu Reagent), methanol (AR, Fuyu Reagent), ethanol (AR, Fuyu Reagent), acetone (AR, Fuyu Reagent). X-ray diffraction (XRD) patterns were obtained using a Bruker (Germany) D8 Advance diffractometer with Cu Kα radiation (λ = 1.5418 Å) from 5º to 40º at 30 kV and 10 mA under a scan rate of 0.02 degree min^{-1}. Thermogravimetric analysis (TGA, METTLER TOLEDO TGA/SDTA851) were performed to analyze the structure with a heating rate of 5 ºC min^{-1} under air atmosphere. Vario MICRO (Elementar, Germany) was used to perform the Elemental analyses (C, H, and N). The N_2 adsorption measurement was performed using Micromeritics ASAP 2420. CO_2, CH_4 and C_2H_6 adsorption measurements were tested on the Micromeritics 3Flex instrument.

Synthesis steps of Hf-MOF

Typically, 0.5 mL of DMF solution with $HfCl_4$ (40.80 mg, 0.10 mmol) and 0.5 mL of DMF solution with 1,3-di(4-carboxyphenyl)benzene (H_2DCPB) (30 mg, 0.10 mmol) were mixed together in a 10 mL glass vial. Following that, adding 0.2 mL of acetic acid and the solution was sealed and heated at 120 ºC for 4 days. The product was collected by centrifugation at 3,000 rpm for 2 min and washed with DMF for several times. After that, the solids were dried at 60 ºC in a vacuum for 12 hours to get the novel MOFs (denoted as Hf-MOF) with a yield of 80%, based on the using amount of H_2DCPB ligands.

X-ray crystallography

Single crystal of $C_{120}H_{72}Hf_6O_{32}$ was obtained via a Bruker Apex II CCD diffractometer using graphite-monochromated Mo-Kα radiation (λ=0.71073 Å) radiation at room temperature. Using Olex 2,[26] the structure was solved with the SHELXT[27] structure solution program using intrinsic phasing and refined with the SHELXL[28] refinement package using least squares minimisation. The final formula of Hf-MOF was defined by combining the crystallographic data, elemental and TGA results. Crystal data, structure refinement and selected bond lengths of the Hf-MOF was displayed in Table S1. The topology of the Hf-MOF was calculated based on the sofeware of TOPOS 4.0.[29]

Gas adsorption and separation

Before the gas adsorption measurements, the samples should be fully activated. To completely remove the guest solvent molecules, the samples were soaked in acetonitrile, and exchanged with fresh acetonitrile for several times in 4 days. Then, before the gas adsorption measurements, the samples were dried using the 'outgas' function of the Micromeritics analyzer for 10 h at 90oC. The N2 adsorption measurements were carried out on a Micromeritics ASAP 2420 instrument. Adsorption measurements of CO_2, CH_4, C_2H_6 were carried out on a Micromeritics 3-Flex instrument.

S2. Calculation procedures of selectivity from IAST

The measured experimental data is excess loadings (q^{ex}) of the pure components CO_2, CH_4 and C_2H_6 for Hf-MOFs, which should be converted to absolute loadings (q) firstly.

$$q = q^{ex} + \frac{pV_{pore}}{ZRT}$$

Here Z is the compressibility factor. The Peng-Robinson equation was used to estimate the value of compressibility factor to obtain the absolute loading, while the measured pore volume of Hf-MOFs are also necessary.

The dual-site Langmuir-Freundlich equation is used for fitting the isotherm data at 298 K.

$$q = q_{m_1} \times \frac{b_1 \times p^{1/n_1}}{1 + b_1 \times p^{1/n_1}} + q_{m_2} \times \frac{b_2 \times p^{1/n_2}}{1 + b_2 \times p^{1/n_2}}$$

Here p is the pressure of the bulk gas at equilibrium with the adsorbed phase (kPa), q is the adsorbed amount per mass of adsorbent (mol kg^{-1}), q_{m1} and q_{m2} are the saturation capacities of sites 1 and 2 (mol kg^{-1}), b_1 and b_2 are the affinity coefficients of sites 1 and 2 (1/kPa), n_1 and n_2 are the deviations from an ideal homogeneous surface.

The selectivity of preferential adsorption of component 1 over component 2 in a mixture containing 1 and 2, perhaps in the presence of other components too, can be formally defined as

$$S = \frac{q_1/q_2}{p_1/p_2}$$

q_1 and q_2 are the absolute component loadings of the adsorbed phase in the mixture. These component loadings are also termed the uptake capacities. We calculate the values of q_1 and q_2 using the Ideal Adsorbed Solution Theory (IAST) of Myers and Prausnitz.
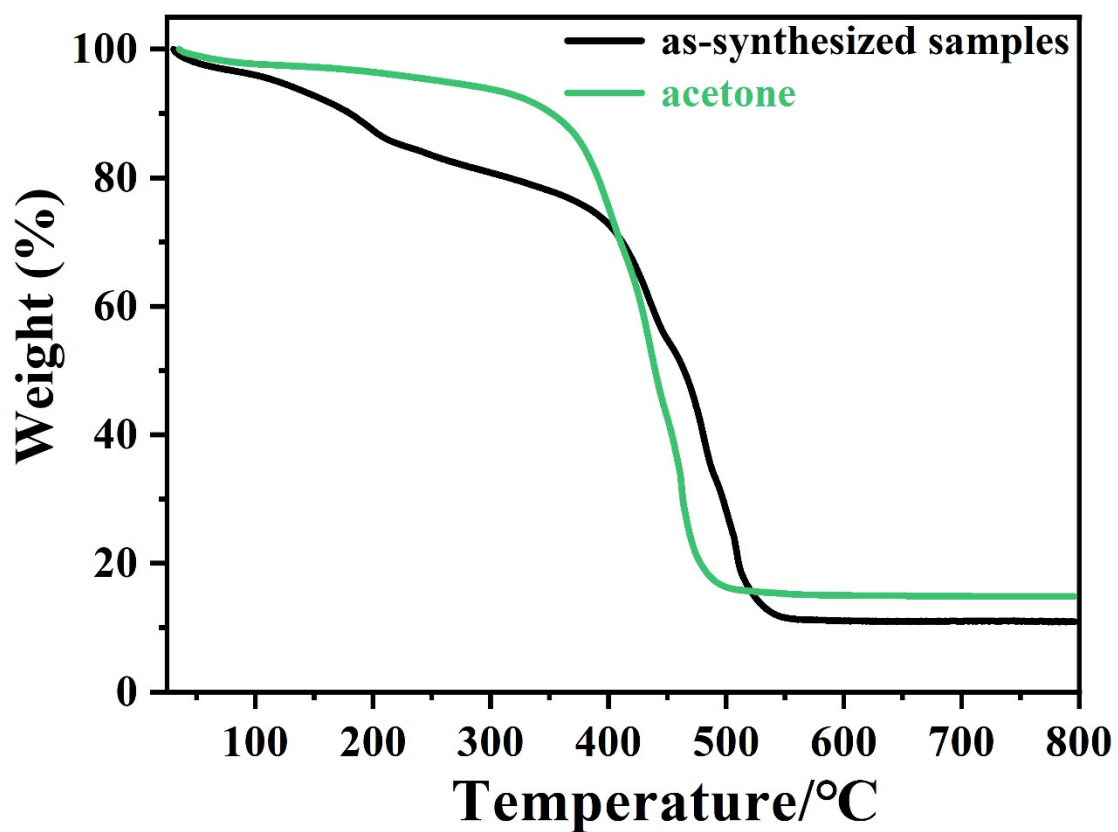
Fig. S1 TGA curve of Hf-MOF for the as-synthesized samples. The high decomposition temperature reveals the notable thermal stability of the Hf-MOF, which can be ssessed by thermo gravimetric analysis under an atmospheric environment.
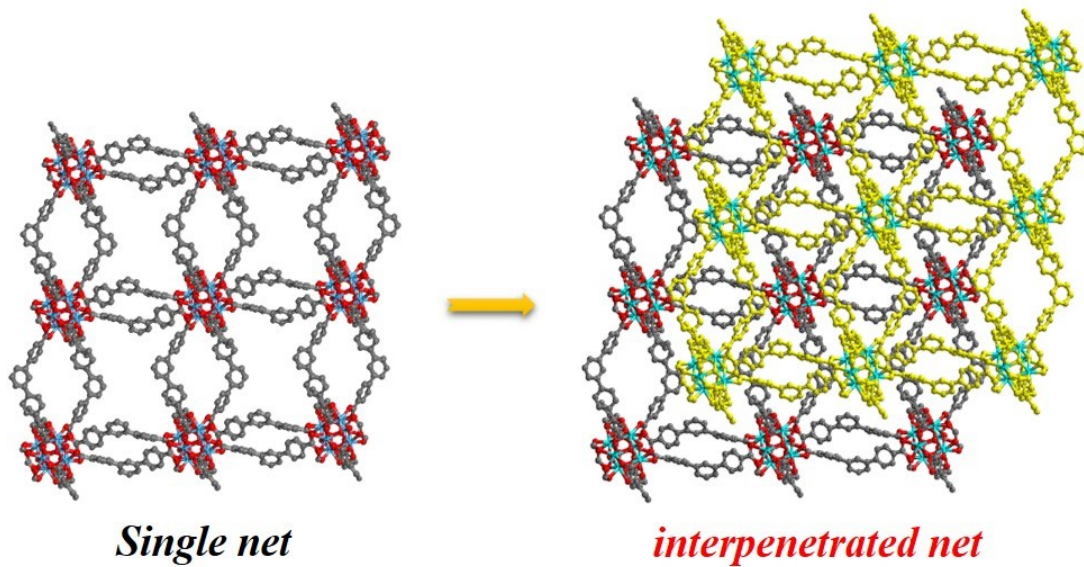
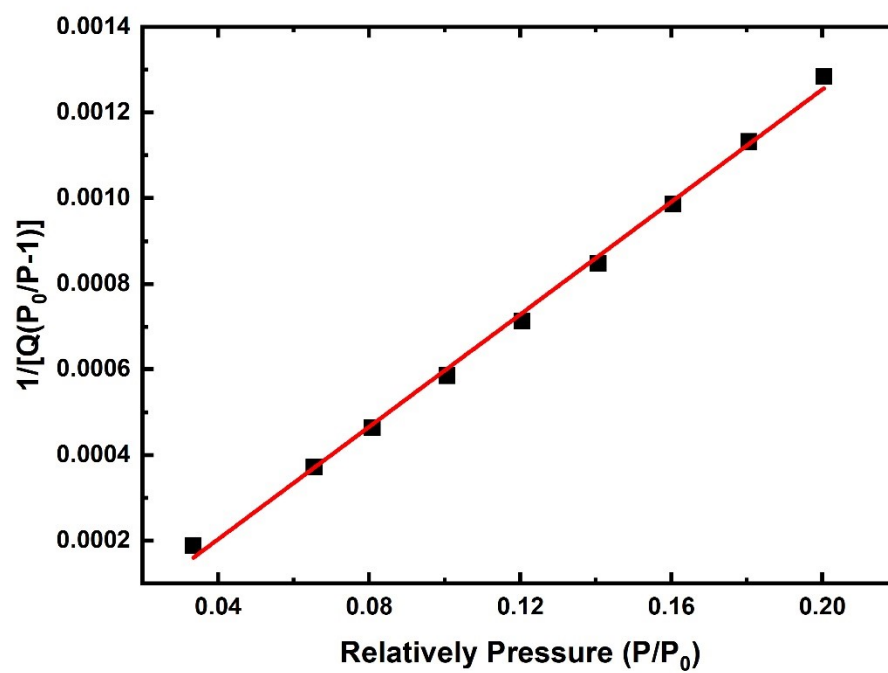**Fig. S2** The single net and interpenetrated net for the framework of Hf-MOF.

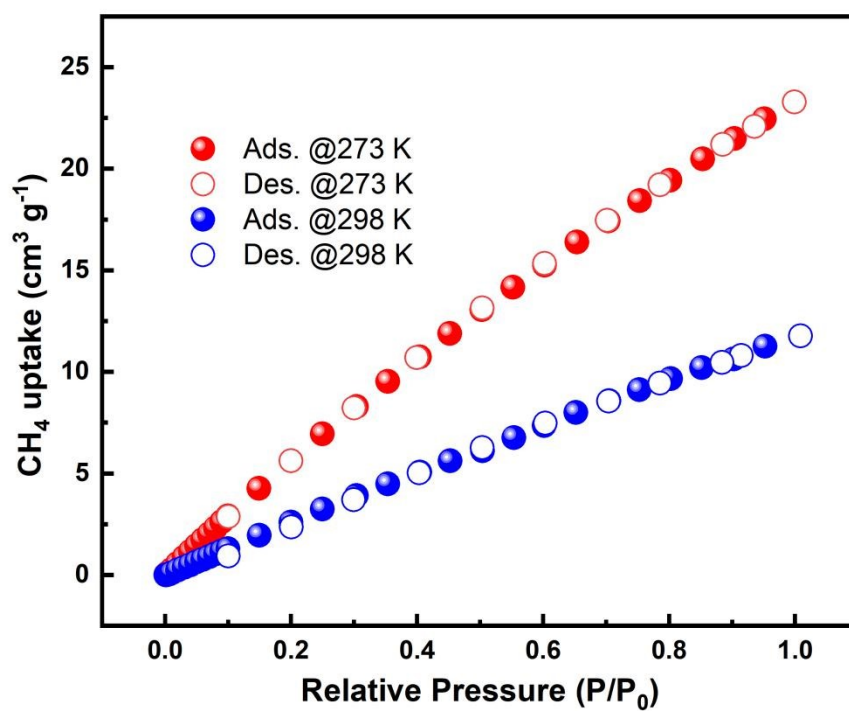**Fig. S3** The linear fitting curve for calculating BET surface areas of Hf-MOF.

Fig. S4 The CH$_4$ isotherms for Hf-MOF at 273 and 298 K under 1 bar.
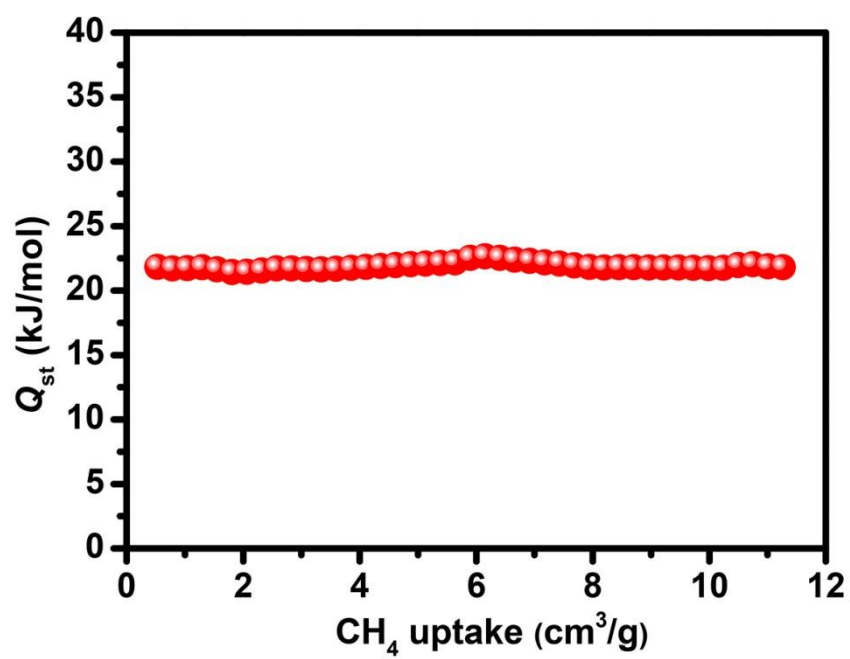
Fig. S5 Q_{st} of CH_4 for Hf-MOF.
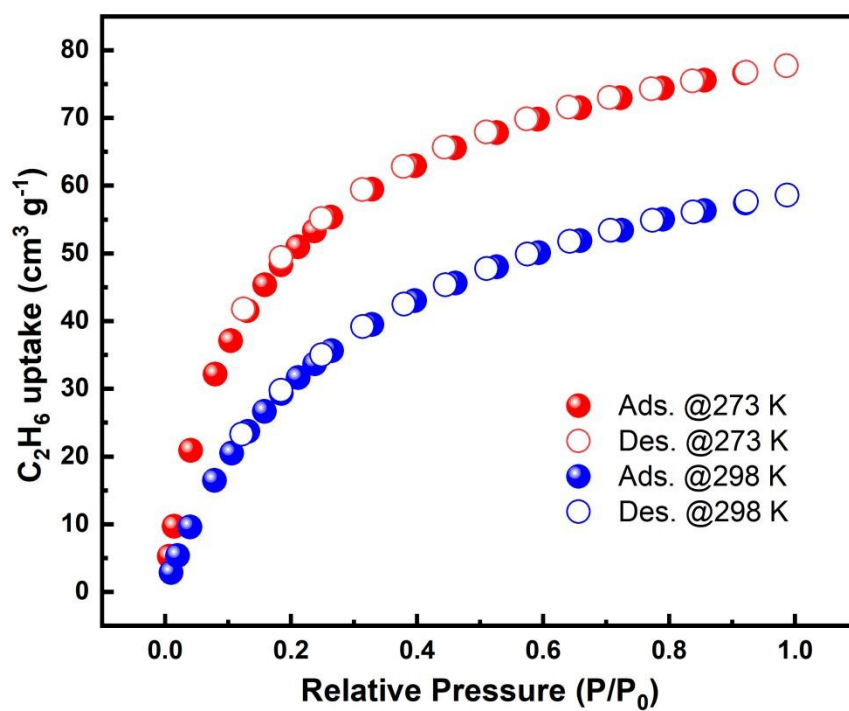
Fig. S6 The C_2H_6 isotherms for Hf-MOF at 273 and 298 K under 1 bar.
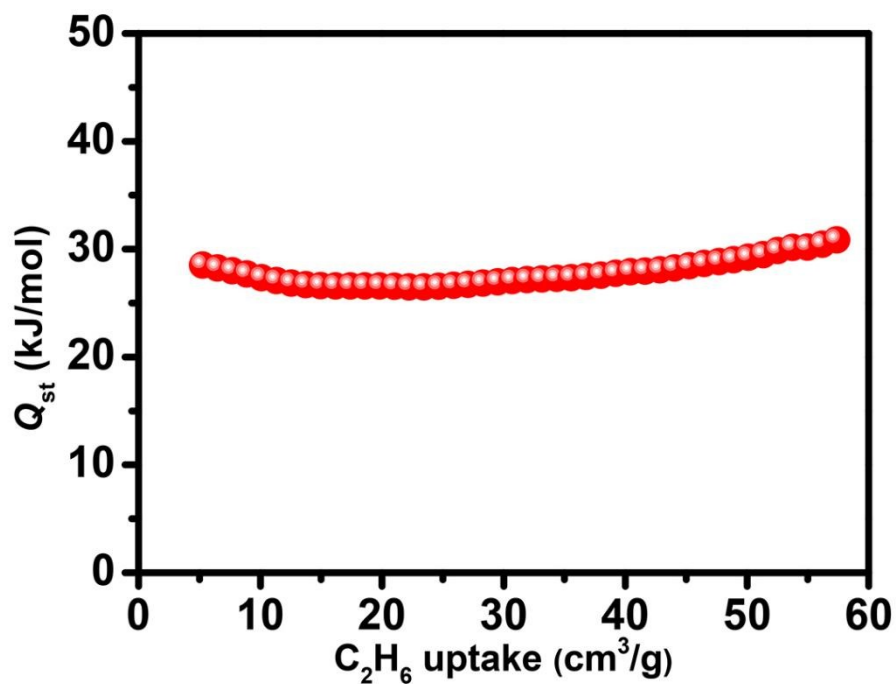
Fig. S7 Q_{st} of C_2H_6 for Hf-MOF. Furthermore, their gas adsorption ability for CH_4 and C_2H_6 were also investigated. As depicted in Fig. S3, the adsorption capacity for CH_4 is 23 and 11 cm^3 g^{-1} at 273 and 298 K under 1 atm, respectively. The adsorption capacity for C_2H_6 is 77 and 58 cm3 g-1 at 273 and 298 K under 1 atm, respectively (Fig. S5). Calculated utilizing the virial model, the Q_{st} values of the Hf-MOF for CH_4 and C_2H_6 were determined to be 20 and 29 kJ mol^{-1}.

Table S1. Selected bond lengths [Å] and angles [°] for **Hf-MOF**.

Hf(1)-O(1)	2.129(4)	C(5)-C(20)	1.464(16)
Hf(1)-O(2)	2.208(7)	C(6)-C(11)	1.403(17)
Hf(1)-O(3)	2.208(8)	C(7)-C(12)	1.351(17)
Hf(1)-O(4)	2.190(7)	C(8)-C(13)	1.376(16)
Hf(1)-O(5)	2.120(9)	C(8)-C(18)	1.413(18)
Hf(1)-O(6)	2.185(8)	C(9)-C(19)	1.390(16)
O(2)-C(4)	1.325(15)	C(9)-C(20)	1.396(17)
O(3)-C(1)	1.335(14)	C(10)-C(14)	1.377(15)
O(4)-C(4)	1.339(15)	C(10)-C(16)	1.338(16)
O(6)-C(1)	1.296(14)	C(11)-C(17)	1.389(17)
C(1)-C(14)	1.509(17)	C(12)-C(17)	1.383(16)
C(2)-C(15)	1.401(17)	C(14)-C(19)	1.357(16)
C(2)-C(18)	1.390(17)	C(6)-C(5)-C(7)	119.6(13)
C(3)-C(11)	1.428(16)	C(6)-C(5)-C(20)	119.1(13)
C(3)-C(13)	1.402(17)	C(16)-C(20)-C(5)	125.6(12)
C(3)-C(15)	1.365(18)	C(14)-C(19)-C(9)	121.2(13)
C(4)-C(18)	1.445(16)	C(2)-C(18)-C(4)	121.1(13)
C(5)-C(6)	1.385(16)	C(12)-C(17)-C(11)	121.5(13)
C(5)-C(7)	1.392(17)	C(8)-C(18)-C(4)	123.4(14)

Table S2. The refined parameters for the Dual-site Langmuir-Freundlich equations fit for the pure isotherms of CO_2, CH_4 and C_2H_6 for Hf-MOF at 298 K.

	q_{m1}	b_1	n_1	q_{m2}	b_2	n_2	R^2
CO_2	2.841272	1.90775	0.01327	0.00144	1.67858	0.91997	0.99998
CH_4	14.62809	1.46471	9.7272E-6	0.01719	1.3754	1.54502	0.99994
C_2H_6	15.22312	0.6929	0.00602	6.0276E-4	0.9391	2.9198	0.99999

Table S3 CO_2 adsorption capacities and Q_{st} values in reported MOFs at 273 K and 1 bar.

MOFs	BET surface area (m^2 g^{-1})	CO_2 uptake (273 K, cm^3 g^{-1})	Q_{st} values (kJ mol^{-1})	Ref.
Hf-MOF	639	65	33	This work
LIFM-28np	940	29.0	22	1
LIFM-79	1689	76.3	32	1
LIFM-77	1619	81.0	34	1
PCN-56	3741	~58	20	2
PCN-57	2572	~50	22	2
PCN-58	2185	~63	24	2
MOF-892	1431	~41	24	3
MOF-893	558	~40	31	3
JLU-MOF58	3663	49	19	4
PCN-138	1261	63	N.A.	5
MIP-203-F	430	61	32	6
MIP-203-S	no	36	34	6
MIP-203-M	380	48	33	6

Table S4. Comparison of CO_2/CH_4 (0.5/0.5) selectivity of Hf-MOF with other MOFs materials.

MOFs material	CO_2/CH_4 selectivity	Ref.
Hf-MOF	6	This work
MOF-177	0.9	7
ZIF-8	1.4	7
Cu$_3$(BTC)$_2$	2.3	7
NOTT-125	4.8	8
FJI-C1	5.9	9
ZJNU-59	6.0	10
NOTT-122	6.4	11
ZJNU-40	6.6	12
ZJNU-69	7.1	13
BSF-1	7.5	14

Table S5. Comparison of C_2H_6/CH_4 (0.5/0.5) selectivity of Hf-MOF with other MOFs materials.

MOFs material	C_2H_6/CH_4 selectivity	Ref.
Hf-MOF	75	This work
$[Cu_2(BTEB)(NMF)_2]\cdot NMF\cdot 8H_2O$	26	15
UTSA-35a	8	16
Cu-TDPAT	18	17
FIR-7a-ht	15	18
JLU-5	18	19
$Cu_2(bada)_2(dabco)$	28	20
UPC-21	15	21
MFM-202a	9	22
S-PI-M-H	19	23
JLU-Liu22	14	24

References

1. C.-X. Chen, Z.-W. Wei, J.-J. Jiang, S.-P. Zheng, H.-P. Wang, Q.-F. Qiu, C.-C. Cao, D. Fenske and C.-Y. Su, *Journal of the American Chemical Society*, 2017, **139**, 6034-6037.

2. H.-L. Jiang, D. Feng, T.-F. Liu, J.-R. Li and H.-C. Zhou, *Journal of the American Chemical Society*, 2012, **134**, 14690-14693.

3. P. T. K. Nguyen, H. T. D. Nguyen, H. N. Nguyen, C. A. Trickett, Q. T. Ton, E. Gutiérrez-Puebla, M. A. Monge, K. E. Cordova and F. Gándara, *ACS Applied Materials & Interfaces*, 2018, **10**, 733-744.

4. X. Sun, J. Gu, Y. Yuan, C. Yu, J. Li, H. Shan, G. Li and Y. Liu, *Inorganic Chemistry*, 2019, **58**, 7480-7487.

5. Y.-C. Qiu, S. Yuan, X.-X. Li, D.-Y. Du, C. Wang, J.-S. Qin, H. F. Drake, Y.-Q. Lan, L. Jiang and H.-C. Zhou, *Journal of the American Chemical Society*, 2019, **141**, 13841-13848.

6. S. Wang, N. Xhaferaj, M. Wahiduzzaman, K. Oyekan, X. Li, K. Wei, B. Zheng, A. Tissot, J. Marrot, W. Shepard, C. Martineau-Corcos, Y. Filinchuk, K. Tan, G. Maurin and C. Serre, *Journal of the American Chemical Society*, 2019, **141**, 17207-17216.

7. Z. Xiang, X. Peng, X. Cheng, X. Li and D. Cao, *The Journal of Physical Chemistry C*, 2011, **115**, 19864-19871.

8. N. H. Alsmail, M. Suyetin, Y. Yan, R. Cabot, C. P. Krap, J. Lü, T. L. Easun, E. Bichoutskaia, W. Lewis, A. J. Blake and M. Schröder, *Chemistry – A European Journal*, 2014, **20**, 7317-7324.

9. Y. Huang, Z. Lin, H. Fu, F. Wang, M. Shen, X. Wang and R. Cao, *ChemSusChem*, 2014, **7**, 2647-2653.

10. Y. Wang, M. He, X. Gao, S. Li, S. Xiong, R. Krishna and Y. He, *ACS Applied Materials & Interfaces*, 2018, **10**, 20559-20568.

11. Y. Yan, M. Suyetin, E. Bichoutskaia, A. J. Blake, D. R. Allan, S. A. Barnett and M. Schröder, *Chemical Science*, 2013, **4**, 1731-1736.

12. C. Song, Y. He, B. Li, Y. Ling, H. Wang, Y. Feng, R. Krishna and B. Chen, *Chemical Communications*, 2014, **50**, 12105-12108.

13. F. Chen, Y. Wang, D. Bai, M. He, X. Gao and Y. He, *Journal of Materials Chemistry A*, 2018, **6**, 3471-3478.

14. Y. Zhang, L. Yang, L. Wang, S. Duttwyler and H. Xing, *Angewandte Chemie International Edition*, 2019, **58**, 8145-8150.

15. X. Yu, Z. Huang, R. Krishna, X. Luo and Y. Liu, *Dalton Transactions*, 2023, **52**, 15101-15106.

16. Y. He, Z. Zhang, S. Xiang, F. R. Fronczek, R. Krishna and B. Chen, *Chemical Communications*, 2012, **48**, 6493-6495.

17. K. Liu, D. Ma, B. Li, Y. Li, K. Yao, Z. Zhang, Y. Han and Z. Shi, *Journal of Materials Chemistry A*, 2014, **2**, 15823-15828.

18. Y.-P. He, Y.-X. Tan and J. Zhang, *Chemical Communications*, 2013, **49**, 11323-11325.

19. D. Wang, T. Zhao, Y. Cao, S. Yao, G. Li, Q. Huo and Y. Liu, *Chemical Communications*, 2014, **50**, 8648-8650.

20. J. Qiao, X. Liu, X. Liu, X. Liu, L. Zhang and Y. Liu, *Inorganic Chemistry Frontiers*, 2020, **7**, 3500-3508.

21. M. Zhang, X. Xin, Z. Xiao, R. Wang, L. Zhang and D. Sun, *Journal of Materials Chemistry A*, 2017, **5**, 1168-1175.

22. S. Gao, C. G. Morris, Z. Lu, Y. Yan, H. G. W. Godfrey, C. Murray, C. C. Tang, K. M. Thomas, S. Yang and M. Schröder, *Chemistry of Materials*, 2016, **28**, 2331-2340.

23. J. Yan, B. Zhang and Z. Wang, *ACS Applied Materials & Interfaces*, 2018, **10**, 26618-26627.

24. D. Wang, B. Liu, S. Yao, T. Wang, G. Li, Q. Huo and Y. Liu, *Chemical Communications*, 2015, **51**, 15287-15289.